REPORT DOCUMENTATION PAGE

Form Approved
OMB No. 0704-0188

1. AGENCY USE ONLY *(Leave blank)*	2. REPORT DATE	3. REPORT TYPE AND DATES COVERED
	October 1998	Annual (23 Sep 97 - 22 Sep 98)

4. TITLE AND SUBTITLE
Role of EGF-related Growth Factor Cripto in Murine Mammary Tumorigenesis

5. FUNDING NUMBERS
DAMD17-96-1-6323

6. AUTHOR(S)
Michael M. Shen, Ph.D.

7. PERFORMING ORGANIZATION NAME(S) AND ADDRESS(ES)
New Jersey University of Medicine and Dentistry
Piscaway, New Jersey 08854

8. PERFORMING ORGANIZATION REPORT NUMBER

9. SPONSORING/MONITORING AGENCY NAME(S) AND ADDRESS(ES)
U.S. Army Medical Research and Materiel Command
Fort Detrick, Maryland 21702-5012

10. SPONSORING/MONITORING AGENCY REPORT NUMBER

11. SUPPLEMENTARY NOTES

12a. DISTRIBUTION / AVAILABILITY STATEMENT
Distribution authorized to U.S. Government agencies only (proprietary information, Oct 98). Other requests for this document shall be referred to U.S. Army Medical Research and Materiel Command, 504 Scott Street, Fort Detrick, Maryland 21702-5012.

12b. DISTRIBUTION CODE

13. ABSTRACT *(Maximum 200*

We are investigating growth factor signaling in the mammary gland through the analysis of *Cripto,* a member of the novel EGF-CFC gene family. Previous studies have suggested that *Cripto* may play an autocrine or paracrine role in human breast tumorigenesis. To determine whether *Cripto* has a causal role in tumorigenesis, and whether it may be involved in normal breast development, we have generated transgenic mice and retroviruses to examine the consequences of *Cripto* overexpression in cell culture and *in vivo*. Our studies have shown that these *Cripto* retroviruses display activity in HC-11 mammary epithelial cells. To analyze receptor binding by CRIPTO protein, we have generated affinity reagents to screen cDNA expression libraries for *Cripto* receptor(s), and have developed an immunoprecipitation assay to detect a cell-surface *Cripto* binding protein. These results demonstrate the feasibility of our approaches to clone the *Cripto* receptor(s).

14. SUBJECT TERMS	15. NUMBER OF PAGES
Breast Cancer mammary gland development transgenic mice; retrovirus; growth factor receptor	22
	16. PRICE CODE

17. SECURITY CLASSIFICATION OF REPORT	18. SECURITY CLASSIFICATION OF THIS PAGE	19. SECURITY CLASSIFICATION OF ABSTRACT	20. LIMITATION OF ABSTRACT
Unclassified	Unclassified	Unclassified	Limited

AD_____

Grant Number DAMD17-96-1-6323

TITLE: Role of EGF-related Growth Factor Cripto in Murine Mammary Tumorigenesis

PRINCIPAL INVESTIGATOR: Michael M. Shen, Ph.D.

CONTRACTING ORGANIZATION: New Jersey Medicine and Dentistry
Piscataway, New Jersey 08854

REPORT DATE: October 1998

TYPE OF REPORT: Annual

PREPARED FOR: U.S. Army Medical Research and Materiel Command
Fort Detrick, Maryland 21702-5012

NOTICE

USING GOVERNMENT DRAWINGS, SPECIFICATIONS, OR OTHER DATA INCLUDED IN THIS DOCUMENT FOR ANY PURPOSE OTHER THAN GOVERNMENT PROCUREMENT DOES NOT IN ANY WAY OBLIGATE THE U.S. GOVERNMENT. THE FACT THAT THE GOVERNMENT FORMULATED OR SUPPLIED THE DRAWINGS, SPECIFICATIONS, OR OTHER DATA DOES NOT LICENSE THE HOLDER OR ANY OTHER PERSON OR CORPORATION; OR CONVEY ANY RIGHTS OR PERMISSION TO MANUFACTURE, USE, OR SELL ANY PATENTED INVENTION THAT MAY RELATE TO THEM.

LIMITED RIGHTS LEGEND

Award Number: DAMD17-96-1-6323
Organization: New Jersey Medicine and Dentistry
Location of Limited Rights Data (Pages):

Those portions of the technical data contained in this report marked as limited rights data shall not, without the written permission of the above contractor, be (a) released or disclosed outside the government, (b) used by the Government for manufacture or, in the case of computer software documentation, for preparing the same or similar computer software, or (c) used by a party other than the Government, except that the Government may release or disclose technical data to persons outside the Government, or permit the use of technical data by such persons, if (i) such release, disclosure, or use is necessary for emergency repair or overhaul or (ii) is a release or disclosure of technical data (other than detailed manufacturing or process data) to, or use of such data by, a foreign government that is in the interest of the Government and is required for evaluational or informational purposes, provided in either case that such release, disclosure or use is made subject to a prohibition that the person to whom the data is released or disclosed may not further use, release or disclose such data, and the contractor or subcontractor or subcontractor asserting the restriction is notified of such release, disclosure or use. This legend, together with the indications of the portions of this data which are subject to such limitations, shall be included on any reproduction hereof which includes any part of the portions subject to such limitations.

THIS TECHNICAL REPORT HAS BEEN REVIEWED AND IS APPROVED FOR PUBLICATION.

_____ 3.26.99

_____ _____

FOREWORD

Opinions, interpretations, conclusions and recommendations are those of the author and are not necessarily endorsed by the U.S. Army.

____ Where copyrighted material is quoted, permission has been obtained to use such material.

____ Where material from documents designated for limited distribution is quoted, permission has been obtained to use the material.

____ Citations of commercial organizations and trade names in this report do not constitute an official Department of Army endorsement or approval of the products or services of these organizations.

MS ✓ In conducting research using animals, the investigator(s) adhered to the "Guide for the Care and Use of Laboratory Animals," prepared by the Committee on Care and use of Laboratory Animals of the Institute of Laboratory Resources, national Research Council (NIH Publication No. 86-23, Revised 1985).

____ For the protection of human subjects, the investigator(s) adhered to policies of applicable Federal Law 45 CFR 46.

MS In conducting research utilizing recombinant DNA technology, the investigator(s) adhered to current guidelines promulgated by the National Institutes of Health.

MS In the conduct of research utilizing recombinant DNA, the investigator(s) adhered to the NIH Guidelines for Research Involving Recombinant DNA Molecules.

____ In the conduct of research involving hazardous organisms, the investigator(s) adhered to the CDC-NIH Guide for Biosafety in Microbiological and Biomedical Laboratories.

Michael Mather 10/21/98

PI - Signature Date

Table of Contents:

5. Introduction:

5.a. Background and significance

5.a.(i) Cripto *encodes a signaling factor with a potential role in breast development and cancer*

Our research on breast development and tumorigenesis centers on the *Cripto* gene, which encodes a secreted growth factor-like molecule with distant similarity to epidermal growth factor (EGF). A role for *Cripto* in human breast cancer has been indicated by previous studies that have shown that *Cripto* is consistently overexpressed in a large percentage of human breast cancers, and is not expressed at high levels in normal breast tissue [1]. Other studies have documented *Cripto* overexpression in human colorectal, gastric, and pancreatic carcinomas [2-4]. Furthermore, overexpression of *Cripto* is able to induce soft agar colony formation by NOG-8 mouse mammary epithelial cells, indicating that *Cripto* has transforming activity [5]. Taken together, these studies have suggested that *Cripto* may be involved in autocrine or paracrine signaling during tumorigenesis.

Several studies have demonstrated that the human CRIPTO protein possesses growth factor activity. First, mitogenic activity has been demonstrated in cell culture experiments using human CRIPTO protein expressed by transfected CHO cells, or a refolded 47-mer peptide that contains the CRIPTO EGF-like motif, both of which can stimulate proliferation of several human breast carcinoma cell lines, including MDA-MB-453 and SK-BR-3 [6]. Secondly, refolded CRIPTO peptide can bind to murine HC-11 mammary epithelial cells and induce tyrosine phosphorylation of the SH2-adaptor protein Shc, resulting in activation of the *ras/raf/MAPK* signaling pathway [7], as well as a phosphatidylinositol 3'-kinase pathway [8]. Finally, treatment of HC-11 cells with CRIPTO protein can block induction of differentiation mediated by lactogenic hormones [8].

Despite the activation of distinct intracellular signaling pathways in response to exogenous CRIPTO protein, the identity of the *Cripto* receptor(s) remains elusive. In particular, the available evidence indicates that CRIPTO, unlike other EGF-related growth factors, interacts with a receptor(s) that is distinct from the four known members of the *erbB* receptor family (EGF receptor, c-*erbB-2/neu/HER-2,* c-*erbB-3,* and c-*erbB-4).* For example, the high-affinity binding of ^{125}I-labeled refolded CRIPTO peptide to HC-11 cells is not competed by *erbB* receptor ligands, and does not stimulate receptor tyrosine phosphorylation in Ba/F3 cells stably transfected with single *erbB* receptor genes or with pair-wise combinations [7]. These and other observations suggest that CRIPTO binds to an as yet unidentified cell-surface receptor(s).

5.a.(ii) Members of the EGF-CFC family have essential and evolutionarily conserved activities

In our previous studies of mesoderm formation during murine development, we isolated a novel gene that we named *Cryptic,* and showed that *Cripto, Cryptic,* and the *Xenopus FRL-1* gene [9] define a new gene family, known as the EGF-CFC family [10]. More recent studies have shown that the zebrafish *one-eyed pinhead (oep)* gene is also a member of this family [11]. The putative protein products of these genes share a potential N-terminal leader sequence, a variant EGF-like motif, a novel conserved cysteine-rich region (the CFC motif), and a C-terminal hydrophobic domain, which may confer association with the cell membrane [10, 11]. Despite their relatively low sequence conservation (about 30% amino acid identity), *Cripto, Cryptic,* and *FRL-1* are all able to rescue the phenotype of *oep* mutant zebrafish embryos [11], demonstrating that EGF-CFC family members have similar biochemical activities.

In recent studies, we have utilized gene targeting ("knock-out") methodology to examine the effects of a null mutation for *Cripto* in mice, and have found that *Cripto* is required for the correct orientation of the anterior-posterior (A-P) axis in the early embryo ([12]; see Appendix). Homozygous *Cripto*$^{-/-}$ embryos generated by targeted gene disruption die shortly after gastrulation at embryonic day 8.5, and display severe defects in formation of the primitive streak and embryonic mesoderm [12]; this also precludes a direct analysis of *Cripto* requirements in mammary gland development. Similarly, *oep* mutant fish display an early embryonic lethal phenotype with profound defects in formation of the prechordal plate, definitive endoderm, and cardiac mesoderm [13]. These early embryonic requirements for *Cripto* in mouse development and *Oep* in zebrafish development suggest that members of the EGF-CFC family interact with an evolutionarily-conserved signaling pathway.

5.b. Scope and purpose of research

In our research supported by USAMRMC Breast Cancer Research Program, we are investigating several fundamental questions regarding a potential role for *Cripto* in breast development and tumorigenesis. First, the current evidence implicating *Cripto* in oncogenesis is indirect, with no causal role for *Cripto* having been demonstrated. Secondly, it remains unclear whether *Cripto* may represent a signaling factor involved in normal growth and differentiation of the mammary gland. Finally, investigation of the molecular mechanisms of *Cripto* action is greatly hampered by a lack of information concerning the *Cripto* receptor(s).

Therefore, to evaluate the putative oncogenic activities of *Cripto,* we have generated *Cripto*-expressing transgenic mice to assay mammary tumorigenesis *in vivo* (*Technical Objective I*). Secondly, we have produced retroviral vectors to investigate the consequences of *Cripto* overexpression in mammary epithelial cell lines that represent model systems for mammary differentiation and tumor progression (*Technical Objective II).* Finally, we have developed reagents and assays that will facilitate the molecular cloning of the *Cripto* receptor(s) *(Technical Objective III).* These studies will permit the biochemical investigation of downstream signal transduction pathways and the cellular and molecular consequences of *Cripto* signaling.

6. Body:

6.a. Materials and methods

6.a.(i) Generation and analysis of transgenic mice

To produce transgenic founder animals, we performed oocyte microinjection using standard techniques [14], in the FVB/N inbred strain [15]. To assay the genotype of the resulting offspring, tail DNA was analyzed for transgene incorporation by Southern blotting. For analysis of *Cripto* expression, ribonuclease protection assays were performed as described [16] on total RNA extracted from dissected mammary tissues at the indicated stages. All mice are maintained under specific pathogen-free (SPF) conditions, using micro-isolator cages, HEPA-filter cage racks, and laminar flow changing hoods.

6.a.(ii) Production of retroviruses for Cripto *expression*

To produce retroviruses that express *Cripto,* we transiently transfected Phoenix A amphotropic packaging cells with *LZRS-pBMN-2* vectors with appropriate inserts [17]. Following transfection, culture supernatants containing retroviral particles were harvested after two days. HC-

11 mammary epithelial cells were infected by incubation with viral supernatants for five hours in the presence of 4 μg/ml polybrene, as described [18]. Differentiation of HC-11 cells using dexamethasone, insulin, and prolactin (DIP) was carried out as previously described [19]. Recombinant murine CRIPTO protein was produced as a secreted glutathione-S-transferase (GST) fusion protein in culture supernatants of Sf9 insect cells, using the pAcSecG2T baculovirus expression vector (Pharmingen). The recombinant fusion protein was purified using glutathione-Sepharose beads (Sigma), followed by cleavage with thrombin to release purified CRIPTO protein.

6.a.(iii) Receptor binding studies

To perform receptor binding experiments, we have produced constructs to express fusion proteins of CRIPTO with human placental alkaline phosphatase (AP) in mammalian cells. COS-7 cells were transiently transfected using Lipofectamine (Gibco), and conditioned media collected three days later for analysis of alkaline phosphatase activity. Cell supernatants were screened in a colorimetric microplate assay for AP activity by measuring the hydrolysis of *p*-nitrophenyl phosphate, with the amount of AP activity defined as the maximum rate of change of $O.D._{405}$/hour under standardized assay conditions [20]. For library screening to clone a putative CRIPTO receptor, we have utilized an E14 rat dorsal root ganglia cDNA library constructed in the COS cell expression vector pMT21 [21]. Pools of approximately 2000 clones were transiently transfected into COS-7 cells, and histochemical screening using the AP-CRIPTO fusion protein was performed at 48 hours following transfection, as described [20].

To investigate protein interactions by immunoprecipitation, we metabolically labeled HC-11 cells using ^{35}S-methionine, and lysed labeled cells with RIPA buffer. For pull-down experiments with AP-CRIPTO fusion protein, we incubated labeled cell lysates with AP-CRIPTO culture supernatant (1000 U/ml), or AP supernatant (1000 U/ml) as a control, followed by addition of monoclonal antibody against AP (Sigma) and formalin-fixed Staph A cells (Calbiochem). After incubation at 4°, cell pellets were washed three times with RIPA buffer and loaded on a 12.5% SDS-PAGE gel for analysis. For pull-down experiments with GST-CRIPTO fusion protein, we incubated cell lysates with 10 μg purified GST-CRIPTO fusion protein, followed by addition of glutathione-Sepharose beads; after incubation, the beads were washed three times with PBS and analyzed by SDS-PAGE. To biotinylate cell-surface proteins, we treated unlabeled HC-11 cells with 0.25 mg/ml sulfo-NHS-LC-biotin (Pierce) as described [22], followed by immunoprecipitation with AP-CRIPTO or control AP supernatants. Immunoprecipitates were resolved by SDS-PAGE, blotted onto PVDF membrane, and detected with avidin-HRP conjugate (Pierce).

6.b. Results and discussion

6.b.(i) Technical Objective I: Generation and analysis of Cripto *transgenic mice*

Rationale: To investigate the effects of *Cripto* on mammary development and oncogenesis, we have generated transgenic mice that overexpress *Cripto* in their mammary glands. We have previously shown that EGF-CFC proteins, including CRIPTO, are poorly secreted from transfected cells in culture, probably because the endogenous signal sequence is non-conventional and directs inefficient secretion ([10]; data not shown). Since the biological activity of a *Cripto* transgene should depend upon the levels of protein secretion attained *in vivo*, we have constructed transgene expression vectors containing either an unmodified (wild-type) *Cripto* gene or a modified *Cripto* gene that should direct high-level protein secretion.

Results: ***(i) Generation of* Cripto *transgenic mice:*** To direct expression of CRIPTO transgenes to the mammary epithelium of transgenic mice, we utilized the *MMTV-SVPA* vector

[23], which contains a mouse mammary tumor virus (MMTV) long terminal repeat (LTR) enhancer/promoter (Figure 1A). We have subcloned mouse *Cripto* cDNAs into this vector, both in unmodified and modified (sec-*Cripto*) forms (Figure 1B). At present, we have successfully generated three founder mice carrying the unmodified *Cripto* transgene, and four founders carrying the sec-*Cripto* transgene. These mice are currently being bred to establish stable lines of transgenic mice, which will be analyzed for transgene expression using ribonuclease protection assays.

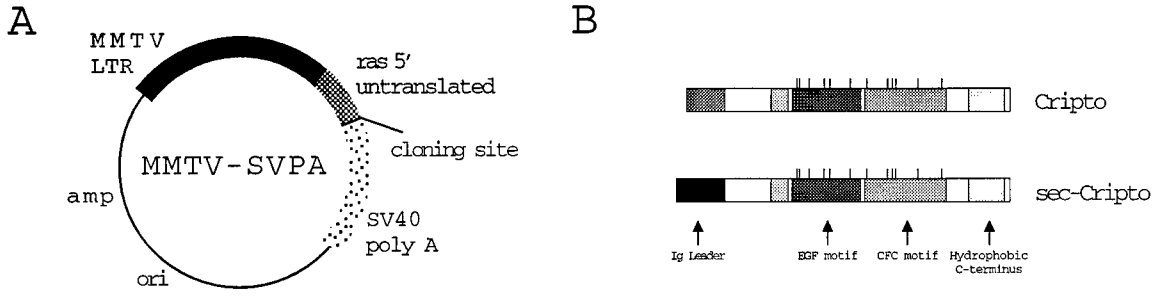

Figure 1. Schematic depiction of the transgene vector and inserts. ***(A)*** **The *MMTV-SVPA* expression vector** contains the long terminal repeat from the mouse mammary tumor virus, 5' untranslated sequences from *ras,* and the 3' polyadenylation region from SV40 [23]. ***(B)*** **The murine *Cripto* transgene inserts** have been produced in unmodifed and modified (Sec-*Cripto*) forms. For the modified construct, we have utilized the leader peptide from a murine immunoglobulin kappa chain gene (from the *pSecTagB* expression vector; Invitrogen) as a replacement for the endogenous CRIPTO leader peptide.

(ii) Analysis of **Cripto** *expression in mammary gland development:* As a first step in investigating the potential activities of *Cripto*, we have examined the expression of the endogenous *Cripto* gene at various stages of mammary development. Previous studies of *Cripto* expression in the mammary gland have utilized a polyclonal antibody directed against the *Cripto* EGF-like domain [24]; however, the interpretation of these studies is complicated by the possibility of cross-reactivity with other members of the EGF-CFC family. Therefore, we have employed RT-PCR and ribonuclease protection assays to examine *Cripto* expression in mammary glands from virgin, pregnant, lactating, and regressing stages. Our results indicate that *Cripto* is expressed at extremely low levels throughout mammary development, with slightly elevated expression during pregnancy and lactation (data not shown).

In current studies, we are employing a different approach to investigate the levels and distribution of *Cripto* transcripts in the mammary gland. For this purpose, we are using our gene targeted mice, which contain a *LacZ* reporter gene "knocked-in" under the transcriptional control of the *Cripto* promoter [12]. We have shown that embryos that are heterozygous for the targeted allele display patterns of *LacZ* expression that are nearly identical to the expression pattern deduced from *in situ* hybridization studies [12]. Consequently, we are now performing β-galactosidase staining of mammary glands of heterozygous *Cripto-LacZ*$^{+/-}$ females at various stages of development, pregnancy, lactation, and regression to examine *Cripto* expression.

6.b.(ii) Technical Objective II: Expression of Cripto *in cell culture model systems*

Rationale: To examine the role of *Cripto* in cellular proliferation, differentiation and transformation, we are utilizing retroviral gene transfer as a strategy to efficiently transfect *Cripto* into relevant cell lines. In our initial studies, we have focused on cell lines that have been reported to respond to exogenous human CRIPTO protein, such as the HC-11 mammary epithelial cell line [7,

8]. Our results form the basis for further studies using other mammary cell lines, as well as mutational approaches to dissect functional domains of the CRIPTO protein.

Results: For efficient gene expression, we have utilized the *LZRS-pBMN-2* retroviral vector, which contains *(i)* full-length Moloney LTRs for efficient gene expression, *(ii)* extended Psi (ψ) sites to direct appropriate packaging of the mRNA, *(iii)* a puromyocin selection marker for enrichment of cells containing the retroviral vector, and *(iv)* Epstein-Barr virus origin and nuclear retention sequences for episomal replication [17]. High-titer retroviral stocks are obtained through transient transfection of the Phoenix packaging cell line, which is a modified 293T cell line derivative that is available for both ecotropic and amphotropic viral production [17]. We have generated *LZRS-pBMN-2* vectors containing murine and human *Cripto* inserts, using either unmodified or modified signal sequences (Figure 1B). Infection of HC-11 and NIH/3T3 cells with these viruses results in high levels of protein production in culture supernatants, as shown by Western blotting with a polyclonal CRIPTO antibody that we have generated (data not shown).

We have used these retroviruses to examine the effects of *Cripto* overexpression upon HC-11 mammary epithelial cells, which can be induced to differentiate by stimulation with lactogenic hormones [19]. This differentiation can be assayed by β-casein production, and can be blocked by addition of exogenous EGF [19]. In addition, we examined the effects of exogenous addition of a recombinant mouse CRIPTO protein that we have produced in Sf9 insect cell supernatants using a baculovirus expression system.

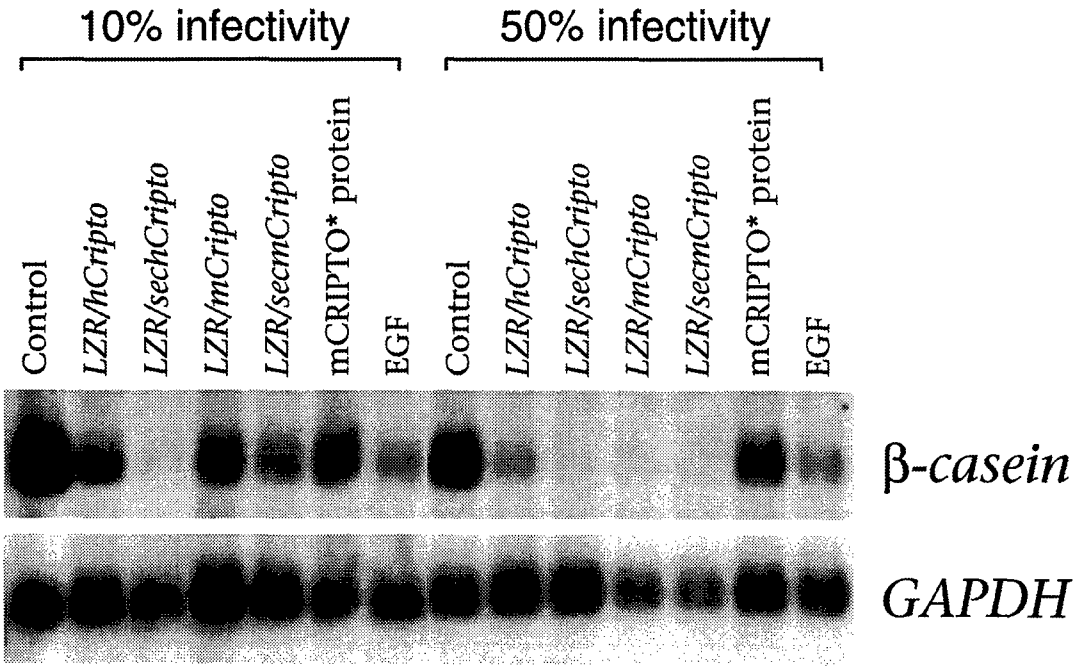

Figure 2. Northern blot analysis of β-casein expression in HC-11 cells. HC-11 cells were infected with the indicated ecotropic retroviruses or were uninfected (control), and induced to differentiate by lactogenic hormones under standard conditions [19]. HC-11 cells were plated at different densities to achieve the indicated percentage of infected cells. For addition of exogenous protein, cells were treated with 10 ng/ml EGF, or treated with 1 ng/ml recombinant CRIPTO protein obtained from insect cell supernatants. 10 μg of total RNA was analyzed by Northern blotting with a β-casein probe, followed by stripping of the filter and re-probing with a *GAPDH* probe as a control for RNA loading.

As seen in Figure 2, infection with viruses expressing mouse or human *Cripto* effectively blocked the differentiation of HC-11 cells, consistent with previous results using continual treatment with exogenous refolded human CRIPTO peptide [8]. Addition of our recombinant purified CRIPTO protein showed a modest effect at the concentration employed. Notably, increased efficiency of secretion through use of the modified leader peptide resulted in more effective inhibition of HC-11 differentiation, implying that CRIPTO protein acts as a secreted product. Furthermore, expression of *Cripto* by a small percentage of cells resulted in a much greater percentage inhibitory effect, suggesting that CRIPTO protein can act on cells other than the ones that produce it (*i.e.*, acts non-cell-autonomously). This observation is of particular importance given that *oep* appears to act cell-autonomously in fish embryos [13]. In ongoing studies, we are constructing retroviruses containing truncated and mutant *Cripto* genes, as well as other members of the EGF-CFC family to begin analysis of functional protein domains.

In other studies, we utilized our *Cripto* retroviruses in studies of focus formation by NIH/3T3 cells, since it had been previously reported that human *Cripto* expression could transform these cells [25]. However, we were unable to reproduce the published results on NIH/3T3 transformation (data not shown), a finding that has been independently confirmed by another laboratory (D. Salomon, personal communication). Therefore, we have now turned to analysis of soft agar plating by NOG-8 mammary epithelial cells, which are partially transformed by *Cripto* overexpression [5]. We will employ the retroviruses that we have generated to examine the transforming activities of *Cripto* in further detail.

6. b.(iii) Technical Objective III: Analysis of CRIPTO binding to cell-surface receptor(s)

Rationale: To investigate CRIPTO protein binding to putative cell-surface receptors, we have generated fusion proteins with secreted human placental alkaline phosphatase (AP), which can be used as soluble affinity reagents [20, 26, 27]. As described in last year's update, we have used this methodology to demonstrate quantitative binding of AP-CRIPTO fusion proteins to MDA-MB-453 and SK-BR-3 mammary carcinoma cell lines, and to show specific patterns of binding to mouse embryo sections. We have now extended these observations in efforts to *(i)* isolate a cDNA clone for a putative receptor by expression library screening and sib selection, and *(ii)* establish direct biochemical assays to identify cell-surface interacting protein(s).

Results: ***(i) Expression library screening:*** Based on our analyses of binding to mouse embryo sections, we found that one of the highest sites of binding was to dorsal root ganglia from 10.5 to 15.5 dpc. This observation was of particular interest since a cDNA expression library from E14 rat dorsal root ganglia had previously been screened successfully using an AP fusion protein reagent [21]. We obtained this library from Dr. Marc Tessier-Lavigne's laboratory for screening with our AP-CRIPTO fusion protein. Out of 60 pools of approximately 2000 clones each, we were able to identify one pool with apparent positive staining, and division of this pool into subpools of approximately 100 clones each has led to identification of two positive subpools. We are currently subdividing these pools to isolate single clones that confer AP-CRIPTO binding.

(ii) Detection of a cell-surface binding protein: As a parallel approach for analysis of the putative *Cripto* receptor(s), we have developed a immunoprecipitation assay for the identification of binding proteins. For this purpose, we have utilized our AP-CRIPTO fusion proteins as affinity reagents to perform pull-down experiments using cell lysates from labeled HC-11 cells. Using metabolically labeled cells, we could specifically immunoprecipitate an approximately 65 kD band and a weaker band with slightly higher electrophoretic mobility from HC-11 cell lysates, but not from culture supernatants (Figure 3A). Notably, these putative interacting proteins were specifically immunoprecipitated by AP-CRIPTO fusion protein, and not by unfused AP protein or by AP fused

to truncated CRIPTO derivatives containing only the EGF or CFC motifs (AP-CRIPTO(EGF) or AP-CRIPTO(CFC)). Furthermore, we have obtained similar results in pull-down experiments using GST-CRIPTO fusion protein produced in Sf9 cell supernatants (not shown).

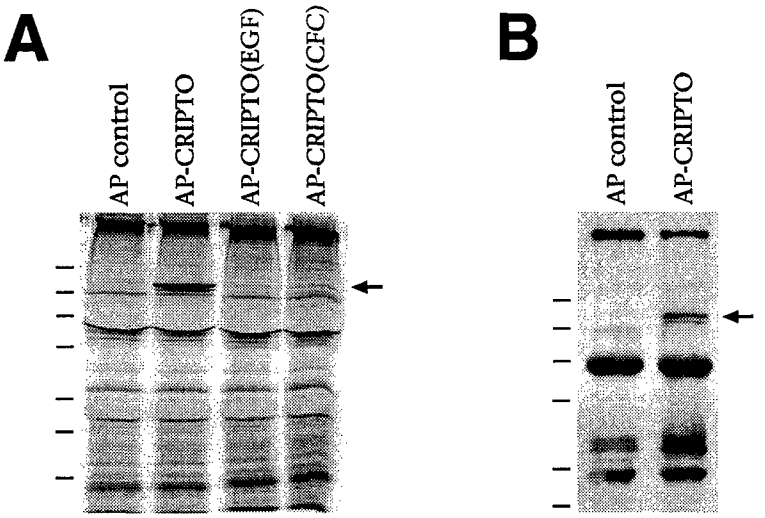

Figure 3. Detection of a cell-surface CRIPTO binding protein. *(A)* HC-11 cells were metabolically labeled with ^{35}S-methionine, and cell lysates were incubated with the indicated proteins produced in COS cell conditioned medium, followed by analysis of immunoprecipitates by SDS-PAGE. Equivalent amounts of AP or AP-fusion protein were used in these pull-down experiments, as demonstrated by Western blotting using an anti-AP antibody (not shown). *(B)* Cell-surface proteins of unlabeled HC-11 cells were biotinylated using sulfo-NHS-LC-biotin reagent, followed by immunoprecipitation and Western blot detection with avidin-HRP. For both panels, lines indicate the positions of molecular mass markers corresponding to 83.6, 61.5, 50.8, 37.6, 25.4, 20, and 14 kDa.

To determine whether these putative interacting proteins are localized to the cell surface, we biotinylated cell-surface proteins on HC-11 cells, and performed a similar pull-down experiment with AP-CRIPTO fusion protein. Again, a band of approximately 65 kD and a weaker 63 kD band could be specifically immunoprecipitated using AP-CRIPTO fusion protein, but not unfused AP (Figure 3B). Similar results were obtained with the MDA-MB-453 and SK-BR-3 mammary carcinoma cell lines (not shown). Thus, we have developed an immunoprecipitation assay that specifically identifies cell-surface proteins that bind to CRIPTO, and are now pursuing biochemical purification of these proteins to perform protein microsequencing.

6.c. Relationship to Statement of Work:

As described above, we have continued to make significant progress towards all three of the Technical Objectives proposed in our original grant application.

For *Technical Objective I*, we have generated transgenic founders expressing murine *Cripto* in the mammary gland, and are now establishing lines of transgenic mice, thereby nearing completion of *Task 1*. We have also initiated studies of endogenous *Cripto* expression in the mammary gland, as a necessary first step in evaluating transgene expression *(Tasks 2, 3)*. These studies should be invaluable in assessing the effects of *Cripto* overexpression upon mammary gland development and tumorigenesis *in vivo*.

For *Technical Objective II,* we have generated retroviruses expressing mouse and human *Cripto,* and have shown that these retroviruses display activity in assays of HC-11 differentiation. Because these retroviruses can be used to infect a wide range of cell types, we have significantly expanded our studies beyond those originally proposed (which only considered MCF-10A cells); thus we have made significant progress towards *Tasks 8-10.* Our continuing studies of HC-11 differentiation and NOG-8 transformation should result in a detailed analysis of *Cripto* activities in mammary differentiation and tumorigenesis using these cell culture model systems.

For *Technical Objective III,* we have previously generated alkaline phosphatase fusion proteins for examination of CRIPTO binding to cell lines and to tissue sections from mouse embryos, thereby completing *Tasks 13-15.* In current experiments, we are screening cDNA expression libraries for clones that bind AP-CRIPTO fusion protein *(Task 17),* and have developed an independent biochemical approach to investigate CRIPTO binding to cell-surface proteins. Thus, we have made substantial progress towards the analysis and future identification of putative *Cripto* receptor(s).

7. Conclusions:

During the past year, we have made significant progress in investigating the activities of *Cripto* in mammary development and tumorigenesis. We have generated several transgenic founder mice containing wild-type and modified transgene constructs that should overexpress *Cripto* in the mammary gland, and have shown that *Cripto* expressing retroviruses are active in an assay of mammary epithelial cell differentiation. Furthermore, we have utilized AP-CRIPTO fusion proteins as affinity reagents to screen cDNA expression libraries for receptor cloning, and to perform immunoprecipitation assays that demonstrate binding to a specific 65 kDa cell-surface protein. Our ongoing studies have demonstrated the feasibility of these approaches for the molecular cloning of the *Cripto* receptor(s).

8. References:

1. Qi, C.F., Liscia, D.S., Normanno, N., Merlino, G., Johnson, G.R., Gullick, W.J., Ciardiello, F., Saeki, T., Brandt, R., Kim, N., Kenney, N., and Salomon, D.S. (1994). Expression of transforming growth factor alpha, amphiregulin and cripto-1 in human breast carcinomas. Br. J. Cancer *69,* 903-910.
2. Kuniyasu, H., Yoshida, K., Yokozaki, H., Yasui, W., Ito, H., Toge, T., Ciardiello, F., Persico, M.G., Saeki, T., Salomon, D.S., and Tahara, E. (1991). Expression of *cripto,* a novel gene of the epidermal growth factor family, in human gastrointestinal carcinomas. Jpn J. Cancer Res. *82,* 969-973.
3. Saeki, T., Stromberg, K., Qi, C.F., Gullick, W.J., Tahara, E., Normanno, N., Ciardiello, F., Kenney, N., Johnson, G.R., and Salomon, D.S. (1992). Differential immunohistochemical detection of amphiregulin and cripto in human normal colon and colorectal tumors. Cancer Res. *52,* 3467-3473.
4. Friess, H., Yamanaka, Y., Buchler, M., Kobrin, M.S., Tahara, E., and Korc, M. (1994). Cripto, a member of the epidermal growth factor family, is over-expressed in human pancreatic cancer and chronic pancreatitis. Int. J. Cancer *56,* 668-674.
5. Ciardiello, F., Dono, R., Kim, N., Persico, M.G., and Salomon, D.S. (1991). Expression of cripto, a novel gene of the epidermal growth factor gene family, leads to in vitro transformation of a normal mouse mammary epithelial cell line. Cancer Res. *51,* 1051-1054.
6. Brandt, R., Normanno, N., Gullick, W.J., Lin, J.H., Harkins, R., Schneider, D., Jones, B.W., Ciardiello, F., Persico, M.G., Armenante, F., Kim, N., and Salomon, D.S. (1994). Identification and biological characterization of an epidermal growth factor-related protein: *cripto-1.* J. Biol. Chem. *269,* 17320-17328.
7. Kannan, S., De Santis, M., Lohmeyer, M., Riese II, D.J., Smith, G.H., Hynes, N., Seno, M., Brandt, R., Bianco, C., Persico, G., Kenney, N., Normanno, N., Martinez-Lacaci, I., Ciardello, F., Stern, D.F., Gullick, W.J., and Salomon, D.S. (1997). Cripto enhances the tyrosine phosphorylation of Shc and activates mitogen-activated protein kinase (MAPK) in mammary epithelial cells. J. Biol. Chem. *272,* 3330-3335.
8. De Santis, M.L., Kannan, S., Smith, G.H., Seno, M., Bianco, C., Kim, N., Martinez-Lacaci, I., Wallace-Jones, B., and Salomon, D.S. (1997). Cripto-1 inhibits β-casein expression in mammary epithelial cells through a $p21^{ras}$- and phophatidylinositol 3'-kinase-dependent pathway. Cell Growth Diff. *8,* 1257-1266.
9. Kinoshita, N., Minshull, J., and Kirschner, M.W. (1995). The identification of two novel ligands of the FGF receptor by a yeast screening method and their activity in Xenopus development. Cell *83,* 621-630.
10. Shen, M.M., Wang, H., and Leder, P. (1997). A differential display strategy identifies *Cryptic,* a novel EGF-related gene expressed in the axial and lateral mesoderm during mouse gastrulation. Development *124,* 429-442.
11. Zhang, J., Talbot, W.S., and Schier, A.F. (1998). Positional cloning identifies zebrafish *one-eyed pinhead* as a permissive EGF-related ligand required during gastrulation. Cell *92,* 241-251.

[redacted]/UNPUBLISHED DATA

12. Ding, J., Yang, L., Yan, Y.-T., Chen, A., Desai, N., Wynshaw-Boris, A., and Shen, M.M. (1998). *Cripto* is required for correct orientation of the anterior-posterior axis in the mouse embryo. Nature *395,* 702-707.

13. Schier, A.F., Neuhauss, S.C.F., Helde, K.A., Talbot, W.S., and Driever, W. (1997). The *one-eyed pinhead* gene functions in mesoderm and endoderm formation in zebrafish and interacts with *no tail.* Development *124,* 327-342.

14. Hogan, B., Beddington, R., Costantini, F., and Lacy, E. (1994). *Manipulating the mouse embryo.* 2nd edition. Cold Spring Harbor Laboratory Press, Cold Spring Harbor, NY.

15. Taketo, M., Schroeder, A.C., Mobraaten, L.E., Gunning, K.B., Hanten, G., Fox, R.R., Roderick, T.H., Stewart, C.L., Lilly, F., Hansen, C.T., and Overbeek, P.A. (1991). FVB/N: an inbred mouse strain preferable for transgenic analyses. Proc. Natl. Acad. Sci. USA *88,* 2065-2069.

16. Shen, M.M., and Leder, P. (1992). Leukemia inhibitory factor is expressed by the preimplantation uterus and selectively blocks primitive ectoderm formation *in vitro.* Proc. Natl. Acad. Sci. USA *89,* 8240-8244.

17. Kinsella, T.M., and Nolan, G.P. (1996). Episomal vectors rapidly and stably produce high-titer recombinant retrovirus. Hum. Gene Ther. *7,* 1405-1413.

18. Cepko, C., and Pear, W. (1996). "Transduction of genes using retroviral vectors", in *Current Protocols in Molecular Biology,* F.M. Ausubel, *et al.*, eds. John Wiley & Sons: New York. pp. 9.91-9.14.6.

19. Hynes, N.E., Taverna, D., Harweth, I.M., Ciardello, F., Salomon, D.S., Yamamoto, T., and Groner, B. (1990). Oncogene transfer into cultured mouse mammary epithelial cells: tumorigenesis and interference with lactogenic hormone action. Mol. Cell Biol. *10,* 4027-4034.

20. Cheng, H.-J., and Flanagan, J.G. (1994). Identification and cloning of ELF-1, a developmentally expressed ligand for the Mek4 and Sek receptor tyrosine kinases. Cell *79,* 157-168.

21. He, Z., and Tessier-Lavigne, M. (1997). Neuropilin is a receptor for the axonal chemorepellent semaphorin III. Cell *90,* 739-751.

22. Altin, J.G., and Pagler, E.B. (1995). A one-step procedure for biotinylation and chemical cross-linking of lymphocyte surface and intracellular membrane-associated molecules. Anal. Biochem. *224,* 382-389.

23. Wang, T.C., Cardiff, R.D., Zukerberg, L., Lees, E., Arnold, A., and Schmidt, E.V. (1994). Mammary hyperplasia and carcinoma in MMTV-cyclin D1 transgenic mice. Nature *369,* 669-671.

24. Kenney, N.J., Huang, R.P., Johnson, G.R., Wu, J.X., Okamura, D., Matheny, W., Kordon, E., Gullick, W.J., Plowman, G., Smith, G.H., Salomon, D.S., and Adamson, E.D. (1995). Detection and location of amphiregulin and Cripto-1 expression in the developing postnatal mouse mammary gland. Mol. Reprod. Dev. *41,* 277-286.

25. Ciccodicola, A., Dono, R., Obici, S., Simeone, A., Zollo, M., and Persico, M.G. (1989). Molecular characterization of a gene of the "EGF family" expressed in undifferentiated human NTERA2 teratocarcinoma cells. EMBO J. *8,* 1987-1991.

26. Flanagan, J.G., and Leder, P. (1990). The kit ligand: a cell surface molecule altered in steel mutant fibroblasts. Cell *63*, 185-194.

27. Cheng, H.-J., Nakamoto, M., Bergemann, A.D., and Flanagan, J.G. (1995). Complementary gradients in expression and binding of ELF-1 and Mek4 in development of the topographic retinotectal projection map. Cell *82*, 371-381.

The supernatants were pre-cleared with Sepharose-4BL beads and immunoprecipitated with anti-Myc-epitope antibody (9E2.10). The immunoprecipitates were then washed twice with RIPA-DOC buffer, resolved by 4–20% SDS–PAGE, and quantified by phosphorimaging with subtraction of individual lane background.

Analysis of PS1-transgenic mice. Wild-type and mutant *PS1* cDNAs were cloned into a Thy-1 expression vector and transgenic mice were generated and bred as described[26]. We identified founders by Southern blotting of genomic DNA from tail biopsies. Transgene-positive offspring were identified by polymerase chain reaction and confirmed by western blotting of cortical homogenates for human PS1 fragments. Transgene expression was also monitored by *in situ* hybridization for the human PS1 messenger RNA.

Quantitative analysis of β-catenin in the human brain. Grey matter was dissected from the temporal cerebral cortex of control cases ($n = 10$, average age 59 years, age range 25–86 years), cases with sporadic Alzheimer's disease ($n = 7$, average age 71, age range 63–82), and cases with familial Alzheimer's disease with PS1 mutations (G209V; $n = 2$; C410Y, $n = 3$; M139I, $n = 2$; H163R, $n = 2$; average age 51, age range 41–59; one case with a C410Y mutation was 84 years old). The tissue was extracted in RIPA-DOC buffer supplemented with protease inhibitors and cleared by centrifugation (100,000*g*, 60 min, 4 °C), and protein-equivalent samples were resolved by 4–20% SDS–PAGE. For detection of β-catenin, samples were heated for 1 min at 90 °C before loading. For detection of PS1, samples were loaded without previous heating. The proteins were electrotransferred to Immobilon-P membrane and immunoblotted with anti-PS1-N (1:5,000) or anti-β-catenin (mAb14; 1:1,000), followed by incubation with ^{125}I-conjugated anti-rabbit or anti-mouse IgG and quantitative analysis by phosphorimaging.

Analysis of neuronal apoptosis. We established and transfected primary cultures of rat E18 hippocampal neurons as described[27]. We added fibrillar amyloid-β protein residues 1–40 (ref. 28) to 40 μM at 12 h after transfection, and incubated the cultures for a further 36 h. Transfected neurons were identified by double labelling for GFP and neuron-specific β-tubulin. Apoptotic neurons were identified by characteristic nuclear morphology after staining with Hoechst 33342 (1 μg ml^{-1}).

Received 10 August; accepted 24 September 1998.

1. Sherrington, R. *et al.* Cloning of a gene bearing missense mutations in early-onset familial Alzheimer's disease. *Nature* **375,** 754–760 (1995).
2. Levy-Lahad, E. *et al.* Candidate gene for chromosome 1 familial Alzheimer's disease locus. *Science* **269,** 973–977 (1995).
3. Rogaev, E. I. *et al.* Familial Alzheimer's disease in kindreds with missense mutations in a gene on chromosome 1 related to the Alzheimer's disease type 3 gene. *Nature* **376,** 775–778 (1995).
4. Li, J., Ma, J. & Potter H. Identification and expression of a potential familial Alzheimer disease gene on chromosome 1 related to AD3. *Proc. Natl Acad. Sci. USA* **92,** 12180–12184 (1995).
5. Zhou, J. *et al.* Presenilin 1 interaction in the brain with a novel member of the Armadillo family. *Neuroreport* **8,** 1489–1494 (1997).
6. Yu, G. *et al.* The presenilin 1 protein is a component of a high molecular weight complex that contains β-catenin. *J. Biol. Chem.* **273,** 164–16475 (1998).
7. Busciglio, J. *et al.* Neuronal localization of presenilin-1 and association with amyloid plaques and neurofibrillary tangles in Alzheimer's disease. *J. Neurosci.* **17,** 5101–5107 (1997).
8. Thinakaran, G. *et al.* Endoproteolysis of presenilin 1 and accumulation of processed derivatives *in vivo*. *Neuron* **17,** 181–190 (1996).
9. Nusse, R. A versatile transcription effector of wingless signalling. *Cell* **89,** 321–323 (1997).
10. Kovacs, D. M. *et al.* Alzheimer-associated presenilins 1 and 2: neuronal expression in brain and localization to intracellular membranes in mammalian cells. *Nature Med.* **2,** 224–229 (1996).
11. Walter, J. *et al.* Alzheimer's disease-associated presenilins are differentially phosphorylated proteins located within the endoplasmic reticulum. *Mol. Med.* **2,** 673–691 (1996).
12. De Strooper, B. *et al.* Deficiency of presenilin-1 inhibits the normal cleavage of amyloid precursor protein. *Nature* **391,** 387–390 (1998).
13. Yankner, B. A. Mechanisms of neuronal degeneration in Alzheimer's disease. *Neuron* **16,** 921–932 (1996).
14. Molenaar, M. *et al.* Xtcf-3 transcription factor mediates β-catenin-induced axis formation in *Xenopus* embryos. *Cell* **86,** 391–399 (1996).
15. van de Wetering, M. *et al.* Armadillo coactivates transcription driven by the product of the *Drosophila* segment polarity gene dTCF. *Cell* **88,** 789–799 (1997).
16. Capell, A. *et al.* The proteolytic fragments of the Alzheimer's disease-associated presenilin-1 form heterodimers and occur as a 100–150-kDa molecular mass complex. *J. Biol. Chem.* **273,** 3205–3211 (1998).
17. Scheuner, D. *et al.* Secreted amyloid beta-protein similar to that in the senile plaques of Alzheimer's disease is increased *in vivo* by the presenilin 1 and 2 and APP mutations linked to familial Alzheimer's disease. *Nature Med.* **2,** 864–870 (1996).
18. Duff, K. *et al.* Increased amyloid-β42(43) in brains of mice expressing presenilin 1. *Nature* **383,** 710–713 (1996).
19. Borchelt, D. R. *et al.* Familial Alzheimer's disease-linked presenilin-1 variants elevate Aβ1-42/1-40 ratio *in vitro* and *in vivo*. *Neuron* **17,** 1005–1013 (1996).
20. Citron, M. *et al.* Mutant presenilins of Alzheimer's disease increase production of 42-residue amyloid beta-protein in both transfected cells and transgenic mice. *Nature Med.* **3,** 67–72 (1997).
21. Morin, P. J., Vogelstein, B. & Kinzler, K. W. Apoptosis and APC in colorectal tumorigenesis. *Proc. Natl Acad. Sci. USA* **93,** 7950–7954 (1996).
22. Ahmed, Y., Hayashi, S., Levine, A. & Wieschaus, E. Regulation of Armadillo by a *Drosophila* APC inhibits neuronal apoptosis during retinal development. *Cell* **93,** 1171–1182 (1998).
23. Wolozin, B. *et al.* Participation of presenilin 2 in apoptosis: enhanced basal activity conferred by an Alzheimer mutation. *Science* **274,** 1710–1713 (1996).
24. Guo, Q. *et al.* Alzheimer's presenilin mutation sensitizes neural cells to apoptosis induced by trophic factor withdrawal and amyloid β-peptide: involvement of calcium and oxyradicals. *J. Neurosci.* **17,** 4212–4222 (1997).
25. Guo, Q. *et al.* Par-4 is a mediator of neuronal degeneration associated with the pathogenesis of Alzheimer disease. *Nature Med.* **4,** 957–962 (1998).
26. Sturchler-Pierrat, C. *et al.* Two amyloid precursor protein transgenic mouse models with Alzheimer disease-like pathology. *Proc. Natl Acad. Sci. USA* **94,** 13287–13292 (1997).
27. Dudek, H. *et al.* Regulation of neuronal survival by the serine-threonine protein kinase Akt. *Science* **275,** 661–665 (1997).
28. Lorenzo, A. & Yankner, B. A. Beta-amyloid neurotoxicity requires fibril formation and is inhibited by Congo Res. *Proc. Natl Acad. Sci. USA* **91,** 12243–12247 (1994).

Acknowledgements. We thank D. Nochlin, C. Lippa, T. Bird, C. Rosenberg, A. Roses, D. Pollin and J. Rogers for autopsy human brain tissue; K. Burki and B. Lederman for assistance in the generation of transgenic mice; and Y. Sun for discussions. This work was supported by grants from the NIH, the Alzheimer's Association and Novartis Pharma Ltd (to B.A.Y.), an NIH training grant and a fellowship from The Medical Foundation (to Z.Z.), a fellowship from the Deutsche Forschungsgemeinschaft (to H.H.), a Pew Scholarship (to X.H.), and an NIH MRRC Core Grant.

Correspondence and requests for materials should be addressed to B.A.Y. (e-mail: Yankner@A1.tch.harvard.edu).

Cripto is required for correct orientation of the anterior–posterior axis in the mouse embryo

Jixiang Ding*, Lu Yang*, Yu-Ting Yan*, Amy Chen†, Nishita Desai*, Anthony Wynshaw-Boris† & Michael M. Shen*

* *Center for Advanced Biotechnology and Medicine and Dept of Pediatrics, UMDNJ-Robert Wood Johnson Medical School, 679 Hoes Lane, Piscataway, New Jersey 08854, USA*

† *Laboratory of Genetic Disease Resarch, National Human Genome Research Institute, 49 Convent Drive, Bethesda, Maryland 20892, USA*

The anterior–posterior axis of the mouse embryo is established by two distinct organizing centres in the anterior visceral endoderm and the distal primitive streak[1–7]. These organizers induce and pattern the head and trunk respectively, and have been proposed to be localized through coordinate cell movements that rotate a pre-existing proximal–distal axis[6,8]. Here we show that correct localization of both head- and trunk-organizing centres requires *Cripto*[9,10], a putative signalling molecule that is a member of the EGF-CFC gene family[11,12]. Before gastrulation, *Cripto* is asymmetrically expressed in a proximal–distal gradient in the epiblast, and subsequently is expressed in the primitive streak and newly formed embryonic mesoderm. A *Cripto* null mutation generated by targeted gene disruption results in homozygous *Cripto*$^{-/-}$ embryos that mostly consist of anterior neuroectoderm and lack posterior structures, thus resembling a head without a trunk. Notably, markers of the head organizer are located at the distal end of the embryo, whereas markers of the primitive streak are absent or localized to the proximal side. Our results indicate that Cripto signalling is essential for the conversion of a proximal–distal asymmetry into an orthogonal anterior–posterior axis.

Members of the EGF-CFC gene family, including *Cripto*, murine *Cryptic*[11], *Xenopus FRL-1*[13], and zebrafish *one-eyed pinhead*[12], encode secreted proteins that contain a divergent epidermal growth factor (EGF)-like motif and a novel cysteine-rich CFC motif[11,12]. EGF-CFC genes are expressed during gastrulation, with limited expression at later embryonic stages, and have been implicated in early development. For example, *FRL-1* has mesoderm and neural-inducing activities in *Xenopus* animal cap assays[13], and *one-eyed pinhead* is required for prechordal plate formation during zebrafish gastrulation[12]. Expression of *Cripto* can be detected in the epiblast

of pre-streak- and primitive-streak-stage embryos[9,10]; Cripto is necessary for cardiogenesis during embryonic stem cell differentiation in culture[14]. We demonstrate here that Cripto is required for early embryogenesis in the mouse, thus establishing an essential role for the EGF-CFC family in mammalian development.

We have found that the expression of *Cripto* during pregastrulation and gastrulation stages is dynamic and is associated with early signs of overt anterior–posterior asymmetry. Before gastrulation, at 5.5 days post coitum (d.p.c.), *Cripto* expression is initially symmetric and uniform in the epiblast, and is not found in the extra-embryonic visceral endoderm (Fig. 1a, b). At 6.0 d.p.c., before primitive streak formation, *Cripto* becomes asymmetrically expressed in the epiblast, in a graded proximal–distal distribution (Fig. 1c–e). By the onset of gastrulation (6.5 d.p.c.), *Cripto* expression localizes to the region of the nascent primitive streak (Fig. 1f–h). In the early stages of gastrulation (6.75 d.p.c.), *Cripto* expression is found in the primitive streak and in the wings of embryonic mesoderm that spread rostrally, while regressing caudally in the epiblast (Fig. 1i, j). During the early neural plate stage (7.25 d.p.c.), expression of *Cripto* fades in the embryonic mesoderm and becomes increasingly confined to the primitive streak and head process (Fig. 1k, l). *Cripto* expression disappears completely by the late neural plate stage (7.75 d.p.c.), whereas a later phase of expression in cardiac progenitors initiates at the late head-fold stage (8.0 d.p.c.) (J.D., H. Wang and M.M.S., unpublished results).

To investigate whether Cripto activity is required for proper gastrulation, we generated a null mutation by targeted gene disruption, simultaneously 'knocking-in' a promoterless *lacZ* marker gene (Fig. 2a). The resulting heterozygous *Cripto*$^{+/-}$ mice are phenotypically normal, and *Cripto*$^{+/-}$ embryos display β-galactosidase staining patterns that resemble those obtained by *in situ* hybridization, albeit with a slight lag in developmental stage that probably reflects protein persistence (Fig. 1m–r). However, homozygosity for the *Cripto* targeted mutation results in embryonic lethality (Fig. 2b). Although no homozygous embryos were obtained after 10.5 d.p.c., *Cripto* homozygotes were recovered in the expected mendelian ratios at 6.75 d.p.c. through to 8.5 d.p.c. (Fig. 2c).

Morphological and histological analysis demonstrated that *Cripto* homozygotes have striking defects in embryonic mesoderm formation and axial organization. The earliest stage at which *Cripto* homozygotes can be reliably distinguished is 6.75 d.p.c., when wild-type littermates are at early-to-mid-streak stages of gastrulation. At this stage, *Cripto* mutants can be identified by the absence of a primitive streak and embryonic mesoderm, and by a thickened layer of visceral endoderm at the distal tip of the egg cylinder (Fig. 2d,h,i). In contrast, in wild-type embryos, the visceral endoderm is thin distally, but is thicker proximally towards the embryonic/extra-embryonic constriction, particularly on the anterior side[2] (Fig. 2d, g). Later, at 7.5 and 8.5 d.p.c. *Cripto* mutants appear to be completely deficient for embryonic mesoderm derivatives such as somites and cardiac tissue, whereas extra-embryonic mesoderm is often formed, including the allantois and blood islands of the visceral yolk sac mesoderm (Fig. 2d–l). Notably, *Cripto* mutant

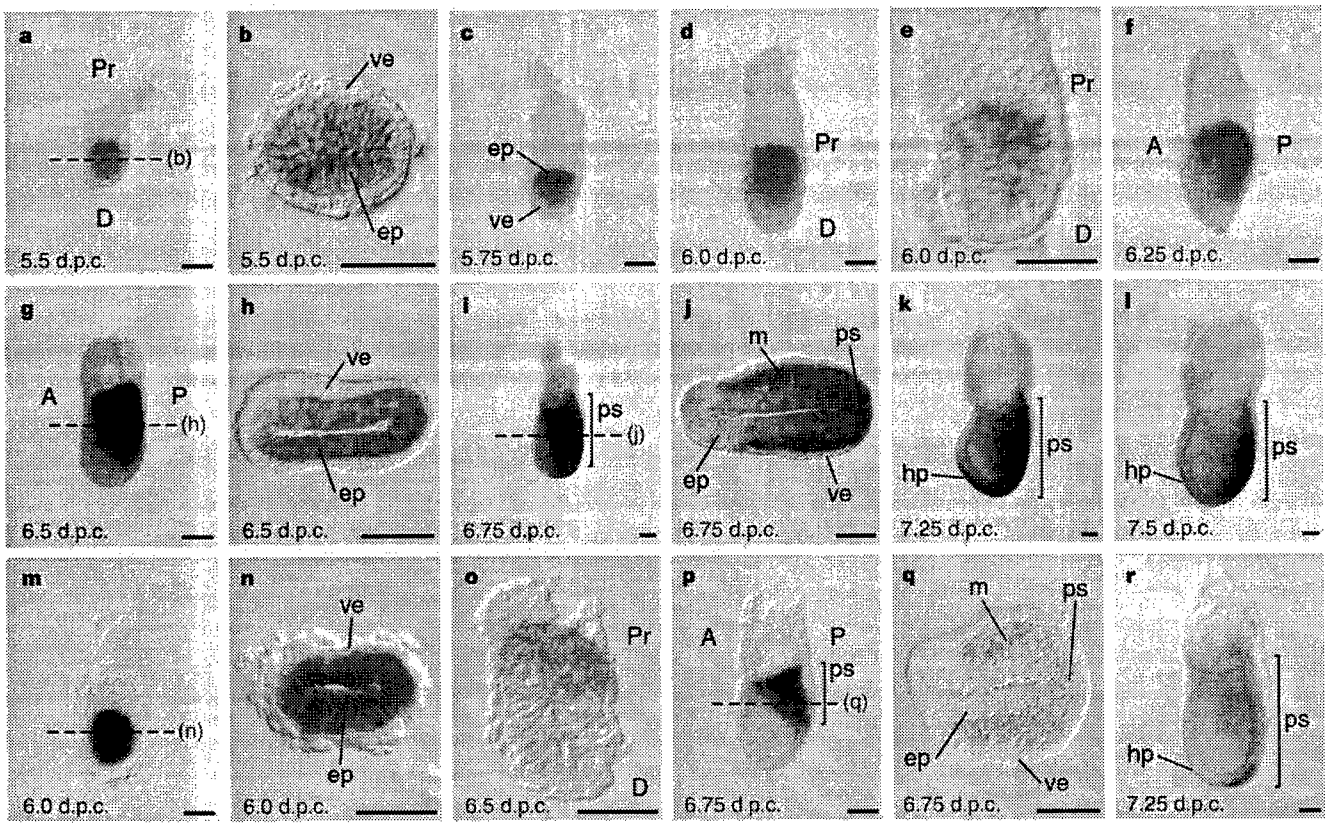

Figure 1 Expression of *Cripto* at pre-gastrulation and gastrulation stages. **a**–**l**, Whole-mount *in situ* hybridization analysis. **a**, Uniform symmetric staining in the epiblast at 5.5 d.p.c.; **b**, a cross section shows lack of expression in the visceral endoderm. **c**, **d**, Proximal–distal gradient of expression in the epiblast. **e**, Sagittal section of **d**. **f**, **g**, Expression shifts caudally before the onset of gastrulation at 6.5 d.p.c. **h**, Cross-section of **g** shows widespread expression in the epiblast and no expression in the visceral endoderm. **i**, Mid-streak stage; **j**, cross-section shows intense staining in the newly formed embryonic mesoderm. **k**, **l**, Expression persists in the primitive streak and head process at the neural plate stage. **m**–**r**, β-Galactosidase staining of *Cripto* heterozygotes. **m**, **n**, Uniform staining in the epiblast before gastrulation. **o**, Sagittal section shows proximal-distal graded staining just before gastrulation. **p**, Early-streak stage embryo, and **q**, cross-section. **r**, Early neural-plate-stage embryo: note more intense staining at distal end of the primitive streak. In all panels, anterior faces to the left when anterior–posterior orientation can be identified; staging before primitive streak formation is approximate. Scale bars, 0.05 mm. A, anterior; D, distal; ep, epiblast; hp, head process; m, mesoderm; P, posterior; Pr, proximal; ps, primitive streak (bar denotes extent of streak); ve, visceral extra-embryonic endoderm.

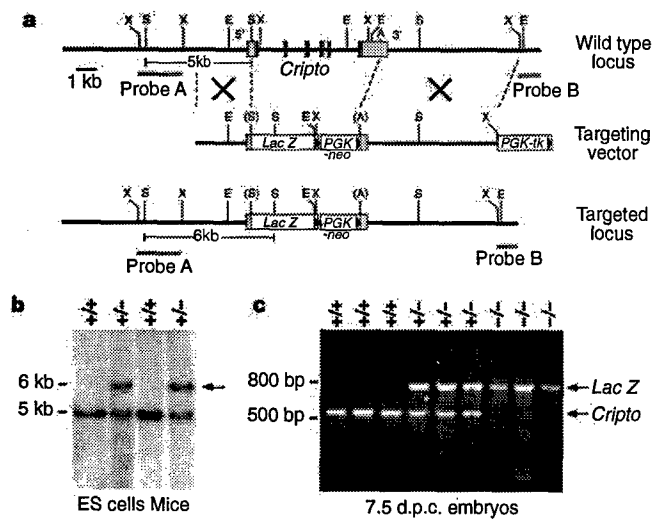

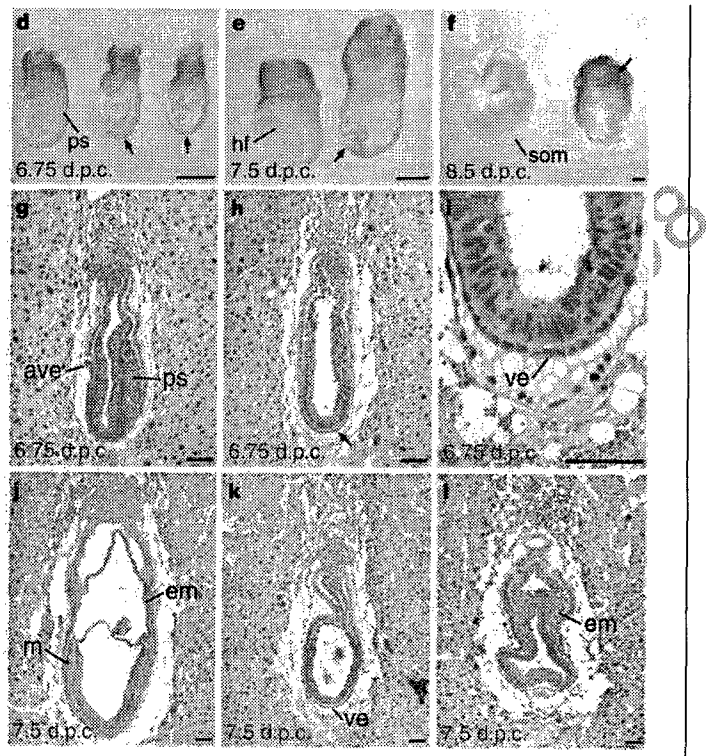

Figure 2 Targeted disruption of *Cripto* and characterization of the null phenotype. **a**, Homologous recombination with the targeting vector deletes the entire *Cripto* coding region (dark boxes), and inserts a promoter-less *LacZ* marker gene into the 5′ untranslated region; triangles indicate orientation of *PGK-neo*, *LacZ*, and *PGK-tk* cassettes. A, *Apa*I, E, *Eco*RI; S, *Ssp*I; X, *Xba*I. **b**, Southern blotting using a 5′ flanking probe (A) detects a 5-kb *Ssp*I fragment in wild-type genomic DNA and a 6-kb fragment (arrow) from the targeted allele in ES cells (lanes 1, 2) and in mice (lanes 3, 4). Targeted ES clones were confirmed using a *LacZ* probe and a 3′ external probe (B) (not shown). **c**, PCR analysis of extra-embryonic tissues demonstrates recovery of wild-type (lanes 1–3), heterozygous (lanes 4–6), and homozygous mutant embryos (lanes 7–9) at 7.5 d.p.c.; the primers amplify a 751-bp *LacZ* fragment and a 536-bp *Cripto* genomic fragment deleted in the targeted allele. **d–f**, Morphology of dissected embryos; scale bars represent 0.2 mm. **d**, Wild-type mid-streak stage embryo at 6.75 d.p.c. (left) and two *Cripto* mutant littermates (centre, right), showing thickened visceral endoderm at the distal tip (arrows). **e**, Wild-type early head-fold embryo at 7.5 d.p.c. (left) and mutant littermate with ectopic ectodermal folds (arrow). **f**, Wild-type embryo at 8.5 d.p.c. (left) and mutant littermate (right), with an apparent blood island in the extra-embryonic region (arrow). **g–l**, Haematoxylin–eosin staining of paraffin sections of embryos within intact decidual tissue at 6.75 d.p.c. (**g–i**) and at 7.5 d.p.c. (**j–l**); scale bars represent 0.1 mm. **g–i**, Wild-type mid-streak embryo (**g**) and *Cripto* mutant littermate (**h**), showing lack of primitive streak and embryonic mesoderm and thickening of the visceral endoderm at the distal tip (arrow), also shown at higher power (**i**). **j–l**, Wild-type neural-plate-stage embryo (**j**) and two *Cripto* mutant littermates, one with no evidence of primitive streak or mesoderm formation (**k**), and the second showing formation of extra-embryonic mesoderm, but not embryonic mesoderm (**l**). Abbreviations: ave, anterior visceral endoderm; em, extra-embryonic mesoderm; hf, head folds; m, embryonic mesoderm; ps, primitive streak; som, somites; ve, visceral endoderm.

embryos have ectopic folds of ectodermal tissue that are located distally, and frequently lack an overt anterior–posterior axis (Fig. 2d–l).

We further characterized the *Cripto* mutant phenotype by examining expression of appropriate marker genes for specific tissues in embryos dissected at 7.5 d.p.c. and 8.5 d.p.c. Consistent with our histological findings, we observed no embryonic expression of *HNF-3β* and *Sonic hedgehog* (*Shh*), which are markers of axial mesoderm and definitive endoderm at these stages (Fig. 3a, b). We also found no evidence for formation of paraxial mesoderm using a *Mox1* probe[15] (Fig. 3c). Similar results were obtained using a *Lim1* probe for caudal lateral plate mesoderm (data not shown). To determine the identity of the ectopic ectodermal folds in *Cripto* mutants, we next investigated the expression of several neuroectoderm markers. In all *Cripto* homozygotes examined, we found widespread expression in the ectoderm layer for *Otx2*, which is initially expressed throughout the undifferentiated epiblast before gastrulation and then marks the prospective forebrain and midbrain at 7.5 d.p.c.[16] (Fig. 3d, e). In addition, expression of the forebrain marker *BF1*[17] was observed in four out of seven embryos at 7.5 d.p.c. and 8.5 d.p.c. (Fig. 3f). *En1*, a marker of prospective midbrain and anterior hindbrain, was expressed in every homozygous embryo examined, usually in an asymmetric patch (Fig. 3g, h). In contrast to these anterior neuroectoderm markers, staining was not observed for *Krox20*, a marker for rhombomeres 3 and 5 of the posterior hindbrain (Fig. 3i). Similarly, expression of the more caudal neural and mesodermal markers *HoxB1* and *HoxB4* was completely absent (Fig. 3j; data not shown). To rule out the possibility that the tissues in *Cripto* mutant embryos correspond to undifferentiated epiblast, we examined expression of the epiblast marker *Oct4* and found no evidence of expression at 7.5 d.p.c. (data not shown). Based on these data, we conclude that *Cripto* mutant embryos are severely deficient for production of embryonic mesoderm and endoderm, and instead largely consist of anterior neuroectoderm.

The absence of embryonic mesoderm and ectopic neuroectoderm in *Cripto* mutants suggested that formation and/or localization of the trunk and head organizing centres might be defective. To determine whether the trunk organizing centre is affected, we used *Brachyury*, an early marker of the primitive streak, and found that it was expressed in a proximal band near the embryonic/extraembryonic constriction at 6.75 d.p.c. (Fig. 3k, l), but was undetectable at 7.5 d.p.c. (data not shown). To confirm this finding, we examined the markers *Fgf8* and *Evx1*, which mark the entire streak and caudal (proximal) primitive streak respectively[18], and obtained similar results at 6.75 d.p.c. (Fig. 3m; data not shown). We also examined expression of *Lim1*, which marks both the primitive

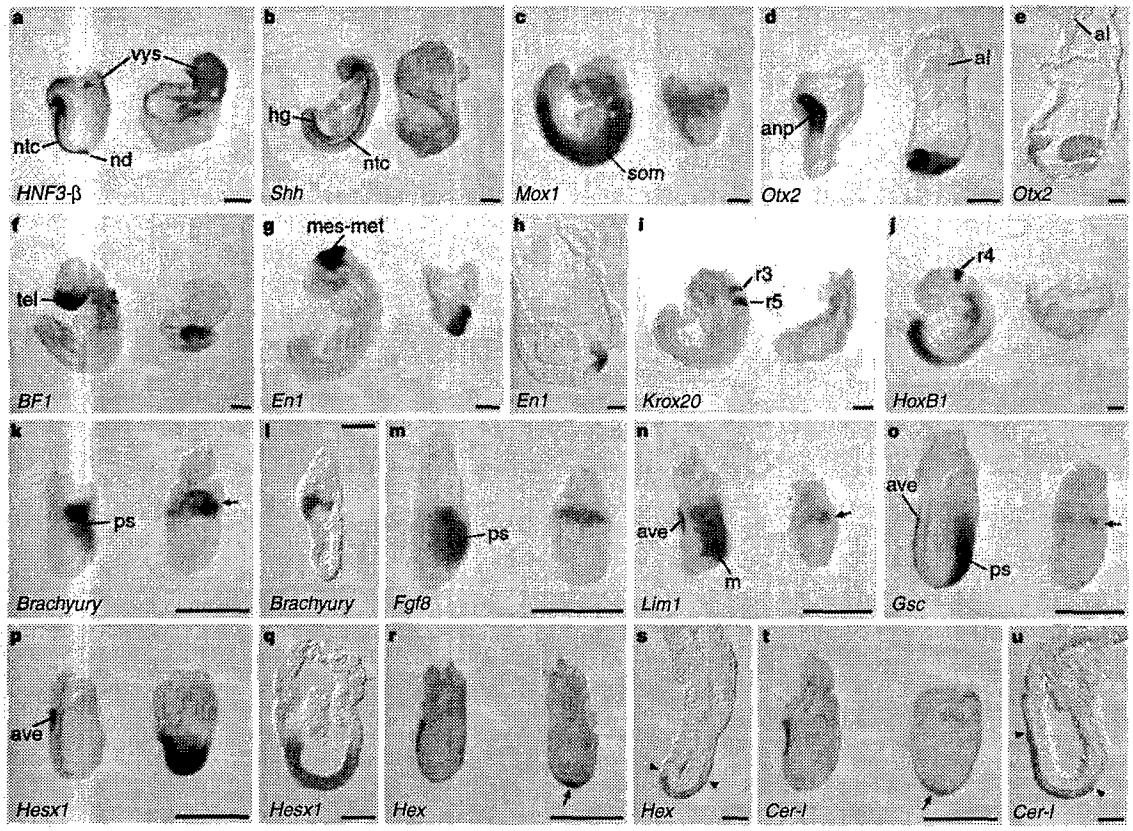

Figure 3 Analysis of marker gene expression. Panels show whole-mount *in situ* hybridization on a wild-type littermate control (left), with anterior facing to the left, and a *Cripto* mutant embryo (right). **a**–**j**, Analysis of embryos at 7.5 (**a**, **d**, **e**) and 8.5 d.p.c. (**b**, **c**, **f**–**j**). **a**, *HNF3-β* is not expressed in the embryonic region of a *Cripto* mutant; weak staining in extraembryonic endoderm of the visceral yolk sac is detected in both embryos. **b**, No expression of *Sonic hedgehog* in a *Cripto* mutant. **c**, *Mox1* expression is not observed in a mutant embryo. **d**, *Otx2* expression in the ectopic distal ectodermal folds of a *Cripto* mutant, also shown in sagittal section (**e**); note the presence of an allantois in the extra-embryonic region. **f**, *BF1* is expressed asymmetrically in a *Cripto* mutant. **g**, *En1* is expressed in the ectodermal folds of a *Cripto* mutant, also shown in sagittal section (**h**). **i**, No expression is detected in *Cripto* mutants for *Krox20*. **j**, No expression is detected in *Cripto* mutants for *HoxB1*, a marker for rhombomere 4 and the posterior neural tube and mesoderm. **k**–**u**, Analysis of embryos at 6.75 d.p.c. **k**, *Brachyury* is expressed in the primitive streak of the wild-type embryo, but in a proximal band in the mutant (arrows), also shown in frontal section (**l**). **m**, *Fgf8* is expressed proximally in a *Cripto* mutant. **n**, Limited proximal expression of *Lim1* in a *Cripto* homozygote (arrow); faint staining in the distal visceral endoderm can occasionally be observed in mutants (not shown). **o**, Faint proximal staining for *Goosecoid* in a *Cripto* mutant (arrow). **p**, Extensive expression of *Hesx1* is observed for all *Cripto* mutants in the ectoderm, as shown by a sagittal section (**q**); weak staining in the visceral endoderm can often be observed but is largely obscured by the ectoderm expression. **r**, *Hex* expression in the thickened visceral endoderm of a *Cripto* mutant; **s**, sagittal section shows the apparent limits of distal staining (arrowheads). **t**, *Cerberus-like* is expressed in the distal visceral endoderm of a mutant embryo (arrow); **u**, frontal section shows that the apparent distribution of staining is broad and asymmetric (arrowheads). Scale bars correspond to 0.2 mm. Abbreviations: al, allantois; anp, anterior neural plate; ave, anterior visceral endoderm; hg, hindgut; m, embryonic mesoderm; mes-met, mesencephalon-metencephalon; ntc, notochordal plate or notochord; nd, node; ps, primitive streak; som, somites; r, rhombomere; tel, telencephalon; vys, visceral yolk sac.

streak and the anterior visceral endoderm[4] (head organizing centre), and observed expression in the proximal epiblast (Fig. 3n). In contrast, expression of *Goosecoid* (*Gsc*), which marks the anterior visceral endoderm and the rostral (distal) region of the primitive streak[3], was absent or appeared in a faint proximal band (Fig. 3o). Similar results were obtained for *HNF-3β*, which is likewise expressed in the anterior visceral endoderm and rostral primitive streak[3] (data not shown). In addition, as *Cripto* expression marks the primitive streak, we performed β-galactosidase staining of mutant embryos at 6.75 d.p.c. and found that staining was always absent (data not shown).

Finally, we investigated whether head organizing activities are affected in *Cripto* mutants by examining several markers that are normally expressed in the anterior visceral endoderm during early gastrulation. Expression of *Hesx1* (also known as *Rpx*), which marks the anterior visceral endoderm and is subsequently induced in the adjacent neuroectoderm[1,19], was found throughout the ectodermal layer of the distal region of the egg cylinder at 6.75 d.p.c. (Fig. 3p, q); this ectopic expression significantly precedes the normal time at which *Hesx1* expression appears in the anterior neural plate of wild-type embryos. This finding suggested that head organizer activity might be mislocalized distally in *Cripto* mutants, which may be consistent with the thickened visceral endoderm at the distal tip (Fig. 2d,h,i). To confirm this, we examined expression of *Cerberus-like* (*Cer-l*), which encodes a candidate head-inducing signal[3,5], and *Hex*, which is the earliest known marker of the prospective head organizer and of anterior–posterior polarity[6]. Both of these genes were expressed in the thickened region of visceral endoderm, with a broad distribution around the distal tip that was sometimes slightly askew (Fig. 3r–u).

In summary, our analysis of *Cripto* mutants indicates that early markers of a head-organizing centre (*Hex*, *Cerberus-like*) are mislocalized in the distal visceral endoderm and, as a result, anterior neuroectoderm is induced distally. In contrast, early markers of the primitive streak (*Brachyury*, *Fgf8*) are mislocalized proximally, whereas little or no expression is observed for later markers of the distal primitive streak (*Goosecoid*, *HNF-3β*), which corresponds to the position of the trunk organizing centre and future node. These

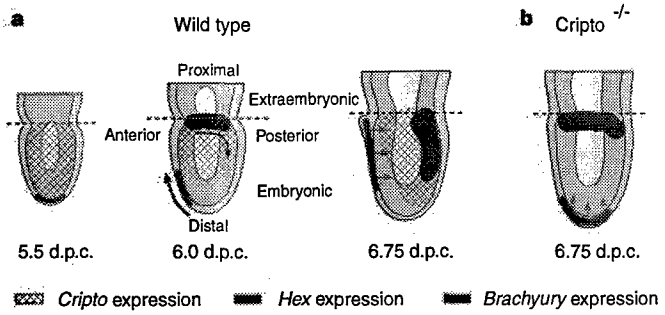

Figure 4 Schematic interpretation of the *Cripto* mutant phenotype. **a**, Model for anterior–posterior axis formation proposed by Beddington *et al.* (adapted from refs 6, 8). Expression of *Hex* (red) and *Brachyury* (blue) correspond to the position of prospective anterior and posterior organizing centres, respectively; orange arrows represent putative head-inducing activities. Also shown is the expression of *Cripto* (hatched) at these stages, based on Fig. 1. Dashed lines indicate the embryonic/extra-embryonic boundary. **b**, Deduced locations of anterior and posterior organizing centres in *Cripto* mutant embryos. We propose that mislocalization of head-organizing activities accounts for the ectopic generation of anterior neuroectoderm in a distal position. Note that loss of *Cripto* activity results in a phenotype in the visceral endoderm, where it is not expressed, consistent with its putative role as a signalling factor, although the basis for this effect may be indirect.

findings correlate with the failure to form embryonic mesoderm, but not extra-embryonic mesoderm, and demonstrate that anterior neural fates can arise in the absence of embryonic mesoderm. Moreover, the lack of posterior neuroectoderm in *Cripto* mutants is consistent with a lack of signals from paraxial mesoderm that are normally required to caudalize neuroectoderm[20]. Consequently, *Cripto* mutant embryos display a 'head-without-trunk' phenotype that is superficially the opposite of that found in mutants for *Otx2* and *Lim1*, which have defects in head-organizing activities[21–23]. Mislocalized distal expression of *Cerberus-like* has been observed in *Otx2* mutants[5], and mislocalized proximal expression of *Goosecoid* in *Otx2*[22] and *Lim-1* mutants[21]; however, these mutants have at least partially intact trunk-organizing activities. Furthermore, the *Cripto* null phenotype also differs from that of *Smad2*, which results in a lack of anterior–posterior asymmetry and no localized expression of markers for both head and trunk organizing centres[7]. Thus, *Smad2* is required for the generation of the anterior–posterior organizing centres, whereas *Cripto* is required for their correct localization.

Our results support a recent model proposed to explain the formation of the anterior–posterior axis in the mouse embryo. Beddington *et al.* have suggested that precursors of the head- and trunk-organizing centres originate on the distal and proximal ends of the pregastrulation embryo, and that vectorial cell movements convert this pre-existing distal–proximal asymmetry into an anterior–posterior axis before gastrulation[6,8] (Fig. 4a). Our findings agree with this model as we found that *Cripto* is required for the correct orientation of the anterior–posterior axis. In particular, our data indicate that rotation of the anterior–posterior axis fails to occur in the absence of *Cripto* activity, resulting in mislocalization of the head- and trunk-organizing centres (Fig. 4b). We suggest that *Cripto* signalling, possibly involving its proximal–distal gradient of expression, is required for the vectorial movements that correctly orient the anterior–posterior axis, and perhaps for coordinating these cell movements in two distinct tissue layers.

Relatively little is known about the signalling activities of EGF-CFC protein products and the molecular identities of their putative receptor(s), although recombinant *Cripto* protein activates the Ras/Raf/MAPK pathway in cultured mammary epithelial cells[24]. Our demonstration of an essential role for *Cripto* in anterior–posterior axis formation underscores the importance of this newly identified family of signalling molecules in vertebrate development. □

Methods

Gene targeting. A partial cDNA corresponding to base pairs (bp) 41 to 985 of the published *Cripto* sequence[9] was amplified by RT-PCR from F9 teratocarcinoma cells, and used to screen a λFIXII library constructed from 129Sv/J genomic DNA (Stratagene). Positive phage clones were screened by PCR to distinguish the authentic *Cripto* locus from pseudogenes[25]. To construct a targeting vector for *Cripto*, a 6.5-kb *Apa*I to *Eco*RI fragment was cloned into the *Bam*HI/*Eco*RI sites of *pPNT*[26] to create the 3′ flank. The 5′ flank was cloned as a 2.6-kb *Xho*I to *Ssp*I fragment cloned into the *Not*I site of *pSDKlacZpA*[27], excised as a *NotI/XhoI* fragment and cloned into the *NotI/XhoI* sites of *pPNT* containing the 3′ flank. Note that the *Ssp*I site of the 5′ arm is located at bp 175 of the *Cripto* cDNA sequence in the 5′ untranslated region. The linearized construct was electroporated into TC1 ES cells[28]; targeted clones were obtained at a frequency of 13% (19/145). ES cell culture and blastocyst injection were done as described[29]. Chimaeric males obtained following blastocyst injection were bred with Black Swiss females (Taconic), and germline transmission was obtained from one targeted ES clone. The targeted mutation has been maintained through backcrossing with outbred Black Swiss mice, and on an inbred 129/SvEv strain background; the phenotype of *Cripto* mutant embryos appears similar in both genetic backgrounds.

Embryo genotyping and phenotypic analysis. Staging of embryos was done according to standard criteria[30]; 0.5 d.p.c. is considered to be noon of the day of the copulatory plug. Embryos analysed at 7.5 d.p.c. and 8.5 d.p.c. were genotyped by PCR using extraembryonic tissues; for 6.75 d.p.c., over 50 embryos have been genotyped, with a strict correlation observed between the genotype and the phenotype described. PCR amplification for genotyping was done at an annealing temperature of 59 °C, using the following primers: for *LacZ*, 5′ CCGCGCTGTACTGGAGGCTGAAG 3′ and 5′ ATACTGCACCGGGCGGGAAGGAT 3′; for *Cripto*, 5′ GCGCACGCTTCCAACTCTACAATC 3′ and 5′ TTCCAAGGCAACCAGGGCTACAC 3′ (corresponding to bp 2,464–2,999 of the genomic sequence[25]). Histological analysis of intact decidua was performed as described[29].

***In situ* hybridization and probes.** Whole-mount *in situ* hybridization was carried out as previously described[11] using the indicated probes, except that embryos were processed in 0.74-μm mesh inserts (Costar) for ease of handling[6]. For each probe, at least five, and usually six or more, *Cripto* mutant embryos were examined at each developmental stage analysed. Whole-mount embryos were stained for β-galactosidase activity as described[27].

Received 8 June; accepted 31 July 1998.

1. Thomas, P. & Beddington, R. S. P. Anterior primitive endoderm may be responsible for patterning the anterior neural plate in the mouse embryo. *Curr. Biol.* **6**, 1487–1496 (1996).
2. Varlet, I., Collignon, J. & Robertson, E. J. *nodal* expression in the primitive endoderm is required for specification of the anterior axis during mouse gastrulation. *Development* **124**, 1033–1044 (1997).
3. Belo, J. A. *et al. Cerberus-like* is a secreted factor with neutralizing activity expressed in the anterior primitive endoderm of the mouse gastrula. *Mech. Dev.* **68**, 45–57 (1997).
4. Tam, P. P. & Behringer, R. R. Mouse gastrulation: the formation of a mammalian body plan. *Mech. Dev.* **68**, 3–25 (1997).
5. Biben, C. *et al.* Murine cerberus homologue mCer-1: a candidate anterior patterning molecule. *Dev. Biol.* **194**, 135–151 (1998).
6. Thomas, P. Q., Brown, A. & Beddington, R. S. P. *Hex*: homeobox gene revealing peri-implantation asymmetry in the mouse embryo and an early transient marker of endothelial cell precursors. *Development* **125**, 85–94 (1998).
7. Waldrip, W. R., Bikoff, E. K., Hoodless, P. A., Wrana, J. L. & Robertson, E. J. Smad2 signaling in extraembryonic tissues determines anterior–posterior polarity of the early mouse embryo. *Cell* **92**, 797–808 (1998).
8. Beddington, R. S. P. & Robertson, E. J. Anterior patterning in mouse. *Trends Genet.* **14**, 277–284 (1998).
9. Dono, R. *et al.* The murine *cripto* gene: expression during mesoderm induction and early heart morphogenesis. *Development* **118**, 1157–1168 (1993).
10. Johnson, S. E., Rothstein, J. L. & Knowles, B. B. Expression of epidermal growth factor family gene members in early mouse development. *Dev. Dyn.* **201**, 216–226 (1994).
11. Shen, M. M., Wang, H. & Leder, P. A differential display strategy identifies *Cryptic*, a novel EGF-related gene expressed in the axial and lateral mesoderm during mouse gastrulation. *Development* **124**, 429–442 (1997).
12. Zhang, J., Talbot, W. S. & Schier, A. F. Positional cloning identifies zebrafish *one-eyed pinhead* as a permissive EGF-related ligand required during gastrulation. *Cell* **92**, 241–251 (1998).
13. Kinoshita, N., Minshull, J. & Kirschner, M. W. The identification of two novel ligands of the FGF receptor by a yeast screening method and their activity in *Xenopus* development. *Cell* **83**, 621–630 (1995).
14. Xu, C., Liguori, G., Adamson, E. D. & Persico, M. G. Specific arrest of cardiogenesis in cultured embryonic stem cells lacking Cripto-1. *Dev. Biol.* **196**, 237–247 (1998).
15. Candia, A. F. *et al. Mox-1* and *Mox-2* define a novel homeobox gene subfamily and are differentially expressed during early mesodermal patterning in mouse embryos. *Development* **116**, 1123–1136 (1992).

16. Ang, S. L., Conlon, R. A., Jin, O. & Rossant, J. Positive and negative signals from mesoderm regulate the expression of mouse Otx2 in ectoderm explants. *Development* **120**, 2979–2989 (1994).
17. Tao, W. & Lai, E. Telencephalon-restricted expression of BF-1, a new member of the HNF-3/fork head gene family, in the developing rat brain. *Neuron* **8**, 957–966 (1992).
18. Crossley, P. H. & Martin, G. R. The mouse Fgf8 gene encodes a family of polypeptides and is expressed in regions that direct outgrowth and patterning in the developing embryo. *Development* **121**, 439–451 (1995).
19. Hermesz, E., Mackem, S. & Mahon, K. A. Rpx: a novel anterior-restricted homeobox gene progressively activated in the prechordal plate, anterior neural plate and Rathke's pouch of the mouse embryo. *Development* **122**, 41–52 (1996).
20. Muhr, J., Jessell, T. M. & Edlund, T. Assignment of early caudal identity to neural plate cells by a signal from caudal paraxial mesoderm. *Neuron* **19**, 487–502 (1997).
21. Shawlot, W. & Behringer, R. R. Requirement for Lim1 in head-organizer function. *Nature* **374**, 425–430 (1995).
22. Ang, S. L. *et al.* A targeted mouse Otx2 mutation leads to severe defects in gastrulation and formation of axial mesoderm and to deletion of rostral brain. *Development* **122**, 243–252 (1996).
23. Rhinn, M. *et al.* Sequential roles for Otx2 in visceral endoderm and neuroectoderm for forebrain and midbrain induction and specification. *Development* **125**, 845–856 (1998).
24. Kannan, S. *et al.* Cripto enhances the tyrosine phosphorylation of Shc and activates mitogen-activated protein kinase (MAPK) in mammary epithelial cells. *J. Biol. Chem.* **272**, 3330–3335 (1997).
25. Liguori, G. *et al.* Characterization of the mouse Tdgf1 gene and Tdgf pseudogenes. *Mamm. Genome* **7**, 344–348 (1996).
26. Tybulewicz, V. L., Crawford, C. E., Jackson, P. K., Bronson, R. T. & Mulligan, R. C. Neonatal lethality and lymphopenia in mice with a homozygous disruption of the c-*abl* proto-oncogene. *Cell* **65**, 1153–1163 (1991).
27. Shalaby, F. *et al.* Failure of blood-island formation and vasculogenesis in Flk-1 deficient mice. *Nature* **376**, 62–66 (1995).
28. Deng, C., Wynshaw-Boris, A., Zhou, F., Kuo, A. & Leder, P. Fibroblast growth factor receptor 3 is a negative regulator of bone growth. *Cell* **84**, 911–921 (1966).
29. Deng, C.-X. *et al.* Murine FGFR-1 is required for early postimplantation growth and axial organization. *Genes Dev.* **8**, 3045–3057 (1994).
30. Downs, K. M. & Davies, T. Staging of gastrulating mouse embryos by morphological landmarks in the dissecting microscope. *Development* **118**, 1255–1266 (1993).

Acknowledgements. We thank C. Abate-Shen, R. Beddington, R. Behringer, E. DeRobertis, A. Joyner, R. Krumlauf, E. Lai, G. Martin, A. McMahon, J. Rossant and C. Wright for gifts of probes and reagents; H. Wang and L. Garrett for technical assistance; and C. Abate-Shen, R. Steward, and members of M.M.S.'s laboratory for advice and comments on the manuscript. This work was supported by a postdoctoral fellowship from the American Heart Association (J.D.), and by grants from the American Heart Association, the U.S. Army Breast Cancer Research Program, and the NIH (to M.M.S.).

Correspondence and requests for materials should be addressed to M.M.S. (e-mail: mshen@cabm.rutgers.edu).

Sexually dimorphic development of the mammalian reproductive tract requires *Wnt-7a*

Brian A. Parr* & Andrew P. McMahon

Department of Molecular and Cellular Biology, The Biolabs, Harvard University, 16 Divinity Avenue, Cambridge, Massachussets 02138, USA

An important feature of mammalian development is the generation of sexually dimorphic reproductive tracts from the Müllerian and Wolffian ducts. In females, Müllerian ducts develop into the oviduct, uterus, cervix and upper vagina, whereas Wolffian ducts regress. In males, testosterone promotes differentiation of Wolffian ducts into the epididymis, vas deferens and seminal vesicle. The Sertoli cells of the testes produce Müllerian-inhibiting substance, which stimulates Müllerian duct regression in males[1–4]. The receptor for Müllerian-inhibiting substance is expressed by mesenchymal cells underlying the Müllerian duct that are thought to mediate regression of the duct[5–7]. Mutations that inactivate either Müllerian-inhibiting substance or its receptor allow development of the female reproductive tract in males[8–12]. These pseudohermaphrodites are frequently infertile because sperm passage is blocked by the presence of the female reproductive system[9,10,12]. Here we show that male mice lacking the signalling molecule Wnt-7a fail to undergo regression of the Müllerian duct as a result of the absence of the receptor for Müllerian-inhibiting substance. *Wnt7a*-deficient females are infertile because of abnormal development of the oviduct and uterus, both of which are Müllerian duct derivatives. Therefore, we propose that signalling by Wnt-7a allows sexually dimorphic development of the Müllerian ducts.

Wnt-7a is a member of the Wnt family of secreted glycoproteins, which function as signalling molecules in several developmental contexts[13]. We have described previously the generation of a mutant *Wnt-7a* allele by homologous recombination in mouse embryonic stem cells[14]. Mice homozygous for the targeted allele exhibit defects in limb patterning, but are otherwise fully viable[14,15]. However, we did not observe pregnancies when homozygous *Wnt-7a*-mutant males or females were mated.

To study the *Wnt-7a*-associated sterility, we dissected the reproductive tracts of postnatal mice. The Müllerian duct derivatives of homozygous *Wnt-7a*-mutant neonate or adult females, as compared with their wild-type or heterozygous littermates, failed to differentiate properly. At the neonatal stage, Müllerian ducts are present but there are no signs of coiled oviducts in homozygous *Wnt-7a*-mutant females (Fig. 1a–c). In addition, the uterine wall is thinner and notably less muscular than that of the wild-type mice (Fig. 1c). Adult *Wnt-7a*$^{-/-}$ females still lack visibly coiled oviducts,

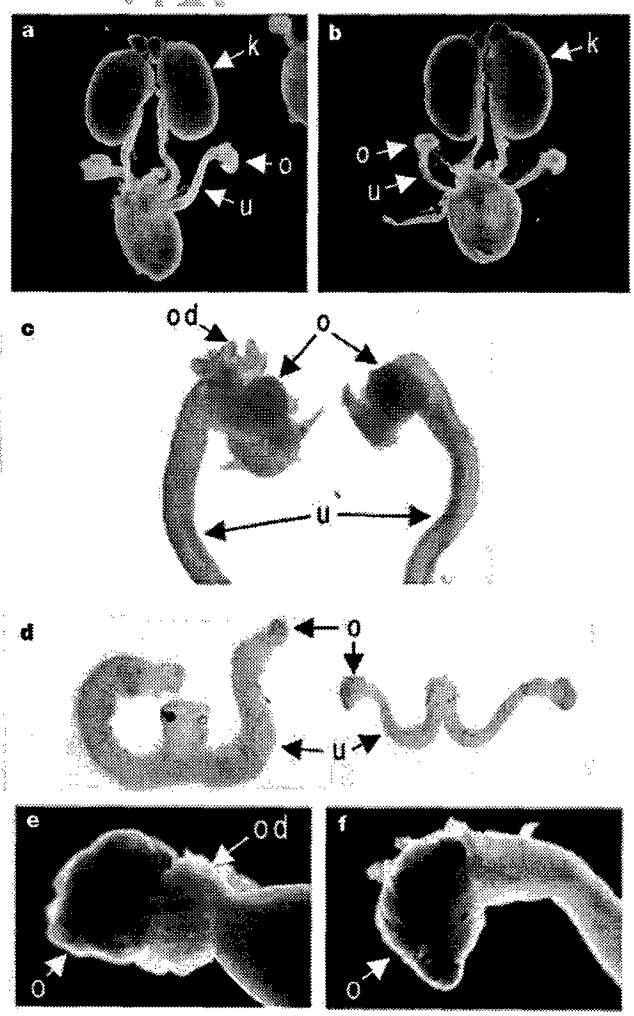

Figure 1 Development of female reproductive tracts in wild-type and *Wnt-7a*-mutant mice. **a**, **b**, The urogenital region of **a**, wild-type and **b**, mutant neonates. k, kidney; o, ovary; u, uterus. **c**, Coiled oviducts (od) are seen in wild-type (left) but not in mutant (right) neonatal mice. The uterus of the mutants is less muscular and more slender than the wild-type uterus. **d**, Adult reproductive tracts of wild-type (left) and homozygous *Wnt-7a*-mutant (right) females. The wild-type uterus is substantially larger and thicker than the mutant uterus. However, ovarian development is similar. **e**, **f**, The coiled oviduct, which is visible in wild-type mice (**e**), is not apparent in *Wnt-7a* mutants (**f**). Comparative photographs of wild-type and mutant siblings in all figures are taken at the same magnification.

* Present address: MCD Biology, University of Colorado, Campus Box 347, Boulder, Colorado 80309, USA.

10/29/2001

DEPARTMENT OF THE ARMY

US ARMY MEDICAL RESEARCH AND MATERIEL COMMAND AND FORT DETRICK
810 SCHRIEDER STREET, SUITE 218
FORT DETRICK, MARYLAND 21702-5000

REPLY TO
ATTENTION OF:

MCMR-RMI-S (70-1y) 17 Oct 01

MEMORANDUM FOR Administrator, Defense Technical Information Center (DTIC-OCA), 8725 John J. Kingman Road, Fort Belvoir, VA 22060-6218

SUBJECT: Request Change in Distribution Statement

1. The U.S. Army Medical Research and Materiel Command has reexamined the need for the limitation assigned to technical reports written for grants. Request the limited distribution statements for the Accession Document Numbers listed at enclosure be changed to "Approved for public release; distribution unlimited." These reports should be released to the National Technical Information Service.

2. Point of contact for this request is Ms. Judy Pawlus at DSN 343-7322 or by e-mail at judy.pawlus@det.amedd.army.mil.

FOR THE COMMANDER:

PHYLIS M. RINEHART
Deputy Chief of Staff for
Information Management

Enclosure